V. Veselý et alii, Frattura ed Integrità Strutturale, 30 (2014) 263-272; DOI: 10.3221/IGF-ESIS.30.33

Focussed on: Fracture and Structural Integrity related Issues

Electrical resistivity and ultrasonic measurements during sequential fracture test of cementitious composite

V. Veselý, P. Konečný, P. Lehner, D. Pieszka, L. Žídek
VŠB-Technical University of Ostrava, Faculty of Civil Engineering, Department of Structural Mechanics, Ostrava, Czech Republic
vesely.v1@fce.vutbr.cz, petr.konecny@vsb.cz, petrlehner@gmail.com, daniel.pieszka@ips-konstrukt.cz, libor.zidek@vsb.cz

ABSTRACT. Cracks in cover of reinforced and pre-stressed concrete structures significantly influence the ingress of deleterious species causing decrease in durability of these structures. The paper is focused on the effect of fracture process on two selected physical parameters of concrete – the electrical resistivity and the ultrasonic pulse passing time – which might be employed as the quality indicator of concrete cover within (non-destructive) procedure(s) of assessment of the structural durability. The concrete electrical resistivity and ultrasonic passing time were investigated here with respect to two variants of treatment of the test specimens' surface (the pre-dried surface and the wet surface). Test configuration of three-point bending of notched beam was utilized to control the crack propagation; the fracture process passed through several loading–unloading sequences between which the electrical resistivity and ultrasonic passing time readings over the fractured region were performed. Equivalent elastic crack model was used for estimation of the fracture advance (described via the effective crack length) at the loading stages corresponding to the resistivity and ultrasonic measurements. Relationships between changes of both the concrete resistivity and ultrasonic pulse passing time and the effective crack length is determined and discussed.

KEYWORDS. Cementitious composite; Three-point bending test; Electrical resistivity; Ultrasound pulse passing time; Effective crack length; Moisture.

INTRODUCTION AND MOTIVATION

The paper is aimed at durability issues of reinforced and pre-stressed concrete civil engineering structures. Service life of such structures is closely connected with the level of their damage caused by initiation and propagation of cracks [1-3]. The manner of their fracture behaviour is referred to as the quasi-brittle one, e.g. [4-6], i.e. there exists a large nonlinear zone around the propagating crack tip where the material is being damaged via numerous failure mechanisms like micro-cracks growth, their coalescence, bending and branching etc., resulting in an increase of porosity of the material in that zone. Aggressive agents (e.g. ice-melting salts, see water etc.) can penetrate to the level of steel reinforcement through the damaged concrete cover more easily. Preferential pathways for the ingress of deleterious species cause decrease in durability of the structures in question which has a considerable economical impact.
In recent years, numerical models taking into account the effect of concrete cracking on the aggressive agents' penetration have been proposed both from the numerical [7,8] and analytical [9,10] standpoint. These models are typically based on

rather significant simplifications concerning description of the physics behind these complex phenomena. Thus, exploring of the effects of cracking on the aggressive agents ingress in more depth seems as very reasonable research issue.
One of procedures for the estimation of concrete ability to resist aggressive agents expressed via diffusion coefficient proposed in literature [11,12] is evaluated through electrical resistivity measurements of concrete. The correlation between the level of concrete cracking and the (change in) electrical resistivity of the material is selected herein as qualitative indicator.
Conducted experiments, whose selected results are presented in this paper, investigate phenomena related to the introduced problem. Evaluation of concrete electrical resistivity complemented with ultrasonic measurements serves as the indicator of the material's ability to resist the penetration of aggressive agent through the material. Observations are performed on both uncracked and cracked specimen regions. Particularly, it is investigated how the aggressive agent ingress can be related to the level of tensile damage of the covering material. In other words, a question relevant for practical interest may sound: How the aggressive agent ingress' increase due to cracking can be estimated (for instance on surfaces of the structural parts under tensile stresses) e.g. even if the damage is not visible by naked eye.
Sequential three-point bending tests of single edge notched concrete beams (SEN-TPB geometry) were performed accompanied with measurement of both the change in electrical resistivity and the decrease of ultrasound pulse velocity in the damaged area. The level of the material damage (the degree of decrease of the material structure's integrity) in the cracked part of test specimens is investigated using ultrasound measurements; changes in electrical resistivity in that part can reveal relationship between the coefficient of diffusion of an aggressive agent (chloride) ions and the extent of the concrete fracture. Both these non-destructive methods are used here with the ambition to employ them for quick assessment of quality of concrete in the tensioned structural regions. This is important with respect to ascertain/eliminate a premature degradation of reinforced and pre-stressed concrete civil engineering structures.
Parts of the study devoted to either the electrical resistivity or ultrasonic measurements were already published by the authors in [13] and [14], respectively; this paper adds new results originating from supplementary tests conducted under different moisture conditions.

EXPERIMENTAL STUDY

Material and specimens

Common concrete mix provided by a local commercial concrete mixing plant was used to produce the test specimens. C 30/37 XF4 ought to be the designed strength class of the used normal concrete. Specimens were casted into steel moulds from one batch of fresh concrete and properly vibrated (for cca 30–60 s). Apart from the standard beams of dimensions $100 \times 100 \times 400$ mm^3 whose test results are reported in this paper also cubes of and cylinders for standard tests on compressive strength, splitting tensile strength and modulus of elasticity (both static and dynamic) were produced. All specimens were submerged in a tank with water at laboratory temperature.
Before fracture tests the beams were cut into three slices (along the longitudinal axe of the beam, in planes perpendicular to the casting direction) by diamond saw. The two cover layers created on the specimens by the bottom of the mould and the upper open surface were also cut off (in a layer of several millimetres) in order to diminish the surface effect (due to the aggregate arrangement and the cement paste layer at the specimen surfaces). Thus, three specimens, marked with letters A, B, C, were prepared from each standard beam, see Fig. 1a). Nominal dimensions of the specimens, $W \times B \times L$ (i.e. width × breadth × length), were equal to $100 \times 30 \times 400$ mm^3. Specimens were then provided with notches, again using the diamond saw.
The tests were conducted in several series, two of which, differing in the moisture treatment of the specimen surfaces, are presented in the paper. The first set of three standard beams, i.e. nine test specimens, was taken out from the curing position in water bath one day before testing. After dividing them into three parts and providing the notches (by diamond saw as well) the surface of the specimens was left at air to dry-out. This specimen set is marked as that with pre-dried surface and consisted of beams marked as T1, T63, and T69. Three slices of each beam, i.e. the test specimens A, B, and C, were provided with notches of relative lengths, α_0, approximately equal to 0.1, 0.3, and 0.5, respectively. The pre-dried surface set was tested at the age of 224 days.
The second set comprising of four standard beams, i.e. twelve test specimens, was cut and notched one day before testing as well and then returned back in the curing bath. Testing was conducted subsequently after taking them out from the bath and letting drip off the water from their surface. However, the surfaces were kept wet during the whole testing procedure treating them by wet sponge. This specimen set is referred to as the wet surface one and consisted of beams

marked as T31, T39, T86, and T88. The test specimens A, B, and C were provided with notches of relative lengths, α_0, approximately equal to 0.25[1], 0.33 and 0.50 respectively. The pre-dried surface set was tested at the age of 1 year.
The loading span, S, of the three-point bending testing configuration was set to 380 mm. Individual dimensions of the tested specimens, their weight and moisture content are given in Tab. 1.

#	part	W [mm]	B [mm]	S [mm]	L [mm]	a_0 [mm]	$\alpha_0 = a_0/W$	M [kg]	θ [%wt.]
Pre-dried Surface Specimens									
T1	A	100.09	26.54	380	400.77	9.52	0.095	2.756	8.16
	B	100.14	27.77	380	400.67	29.70	0.297	2.493	6.47
	C	100.21	30.82	380	400.63	50.48	0.504	2.756	5.80
T63	A	100.15	24.69	380	400.39	9.80	0.098	2.268	5.80
	B	100.10	24.62	380	400.46	30.12	0.301	2.184	6.98
	C	100.04	24.89	380	400.50	49.38	0.494	2.141	7.24
T69	A	100.06	26.33	380	400.01	8.41	0.084	2.332	6.70
	B	99.89	26.44	380	399.93	28.88	0.289	2.369	6.57
	C	99.83	29.17	380	399.93	50.00	0.501	2.597	5.77
Wet Surface Specimens									
T31	A	100.09	29.55	380	400.47	25.62	0.256	2.579	8.95
	B	100.11	29.81	380	400.31	32.07	0.320	2.68	7.50
	C	100.25	32.96	380	400.20	48.85	0.487	2.987	7.10
T39	A	99.62	99.62	380	400.15	25.44	0.255	2.702	8.73
	B	99.54	29.77	380	400.10	31.05	0.312	2.643	7.73
	C	99.57	31.46	380	400.01	47.72	0.479	2.807	7.56
T86	A	100.14	25.74	380	399.79	24.86	0.248	2.324	*4.57
	B	100.21	27.90	380	400.03	32.84	0.328	2.563	*4.06
	C	100.20	26.52	380	400.05	49.84	0.497	2.384	*4.01
T88	A	100.22	29.30	380	400.78	24.44	0.244	2.599	8.26
	B	100.29	29.02	380	401.44	33.09	0.330	2.629	7.06
	C	100.21	32.21	380	401.62	49.44	0.493	2.967	6.76

Table 1: Specimen dimensions, values of relative crack length, mass and moisture.

Fracture testing

Specimens were loaded under control of displacement of the upper jaw at the rate of 0.5 mm/min using Heckert FP 10/1 testing machine. The loading force and the doubled mid-span deflection were recorded using the fixture enabling the pure beam deflection reading, see Fig. 1b).

[1] It was observed during the fracture testing of the first set that the behaviour of specimens with the shortest notches was accompanied with a part of a fast unstable regime where the structural response was not recorded. These parts of the load–deflection diagrams were then reconstructed/approximated. This observed phenomenon is linked to the insufficiently low stiffness of the used testing device. Therefore, deeper notches (causing lower stiffness of the specimens) were used in the second set.

a)

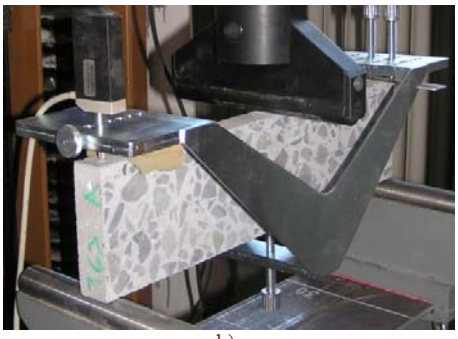

b)

Figure 1: a) Preparation of notched specimens for bending test from standard beams, b) employed fracture test geometry – three-point bending of notched beam – with a depiction of the measuring fixture enabling recording of pure beam deflection.

Several loading–unloading cycles were accomplished during the test on each specimen. Unloading was performed on the beginning of the descending branch of the recorded load–deflection (*P*–*d*) curve (at a value of approx. 80% of the peak load from the corresponding loading cycle). The unloading was performed manually by switching the regime of the used electro-mechanical testing machine. Manual switching didn't allow precise attaining of the desired unloading level, especially in the cases of specimens with the shortest notches (particularly in the pre-dried sample set with $\alpha_0 = 0.1$, see the footnote above). A dynamic onset of fracture (a fast release of energy accumulated in the insufficiently stiff loading system) was observed during the tests of these specimens. This dynamic event was indicated by sparse occurrence of points on a relatively long section of the descending branch of the plotted *P*–*d* diagram. The specimens were removed from the testing machine after full unloading of each cycle. The ultrasound as well as resistivity measurements were conducted (see the subsections bellow) and then the specimens were returned back to the loading machine for the next cycle. The number of cycles varied from two to five depending on the above-mentioned stability of the test (from the perspective of the ability to record the descending branch of the loading curve). Typical examples of *P*–*d* diagrams corresponding to tests with the quasi-static (desired) and dynamic (undesired) fracture are shown in Fig. 2 (the above-mentioned partial approximations of the descending branch of the *P*–*d* curve can be seen in the latter case). The individual loading–unloading cycles are distinguished with colours and marked with Arabic numerals after dash.

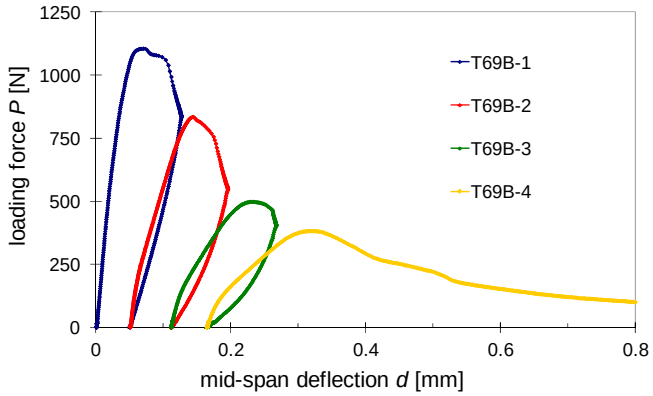

a)

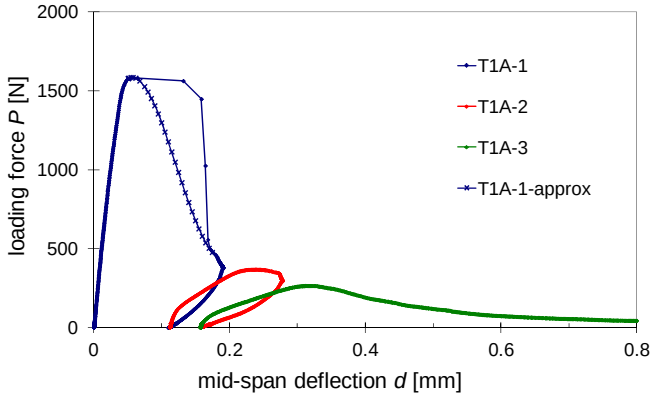

b)

Figure 2: Example of recorded load vs. mid-span deflection curves (*P*–*d* diagrams); a) with quasi-static fracture propagation (specimen T69B), b) with a dynamic event on the descending branch of the first loading cycle (specimen T1A).

Electrical resistivity measurements

Measurements of electrical resistivity, ρ [kΩcm], were conducted on the specimens before starting of the SEN-TPB test and after its individual subsequent unloading stage – the specimens were removed from the loading machine and investigated using the RESI resistivity meter (Proceq). The measurement is conducted via a beam-shaped probe using this apparatus; there are four electrodes placed along the probe (usually referred to as the Wenner probe) perpendicularly to its longitudinal axe. Wet sponges assured the contact between the electrodes of the measuring probe and concrete of the

specimen. The resistivity was measured in three areas along the specimen length − in the left (marked as L), middle (M, i.e. across the fractured cross-section) and right (R) part, respectively[2]. Three readings were made also along the specimen width − near the upper surface of the specimen (the ligament, marked as l), in the middle (m) and near the bottom surface provided with the notch (n)[3]. All these readings were made from either flat side surface of the specimen. The placement of the four electrodes (with wet sponges) of the probe on the specimen surfaces is depicted in Fig. 3a) using circles, the measuring position (M-n) on the front surface is indicated by red colour.

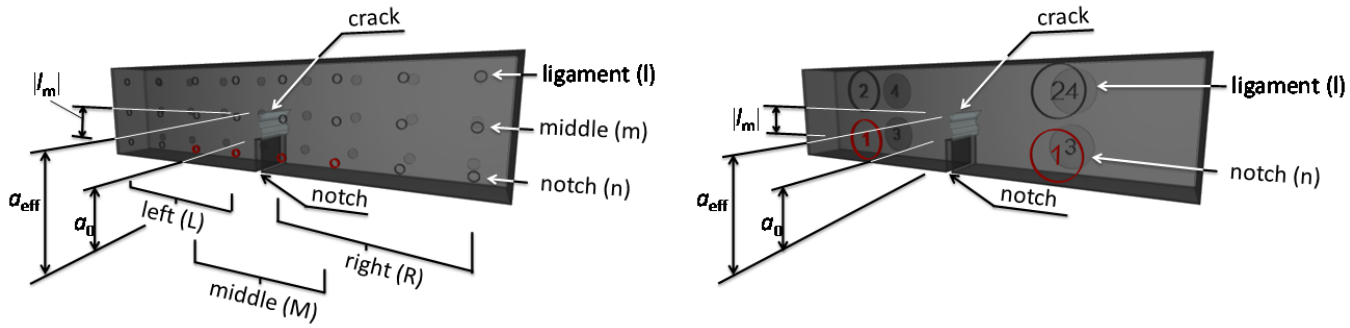

a) b)

Figure 3: Illustration of positioning of probes of the measuring devices on the test specimen in the case of electrical resistivity measurements (a) and the ultrasonic measurements (b).

Ultrasonic measurements

Similarly to the resistivity measurements described above, the concrete specimens were subjected to ultrasonic measurements before each sequence of loading cycle. The TICO ultrasonic instrument (Proceq) was used; this device is able to record the time needed for ultrasound pulse to pass through the defined portion of the concrete test specimen or, inversely, the speed of the ultrasound wave propagation. There are two probes applied on the surface of the test (in our case notched/cracked) specimen, first of which emits and the second receives the ultrasound waves.

The specimens were laid down on a rubber pad in a precisely determined position in order to hold uniformity of placements of the measuring probes at the determined points on the specimen surfaces for measurement of each test specimen. Four points on each side surface, i.e. eight points on both sides, determined the position of the probes for the measurement[4]; see the circles in Fig. 3b). Thus, the pair of measuring probes was placed on two locations on either side of the specimen, at the notch (n) and ligament (l) area (i.e. positions 1, 3 and 2, 4, respectively) Then, the time for the acoustic pulse to pass the sample, t [μs], was measured.

PROCESSING OF RECORDED DATA, USED METHODS AND MODELS

Estimation of current crack length – Effective crack model

The crack length at the stages of test corresponding to the electrical resistivity and ultrasonic measurements were calculated using equivalent elastic crack approach. According to this approach the nonlinear fracture of quasi-brittle material is simulated by replacing the real body containing a crack of a certain length and a fracture process zone ahead of it with a brittle body with an effective crack (longer than the initial one). Both bodies are forced to exhibit the same stiffness parameters (for more details see e.g. [4-6]).

[2] By coincidence, the Wenner probe of the used RESI apparatus was roughly of the same length as one half of the test specimen, so (L) and (R) measurements took place just (centred) at the left and right halves of the specimen, and the (M) measurement over the inner two quarters (the centre of the specimen).

[3] Resistivity measurement locations were distributed along the specimen width, W, as follows: the (n) reading was made at 1/6 of W from the bottom, the (m) one in the middle, and the (l) one at 5/6 of W from the bottom.

[4] The probes of the used TICO instrument are of cylinder shape, cca 50 mm in diameter. The individual probes of the measuring pair were placed at distances 1/4 and 3/4 of the specimen length, L, respectively; (n) measurement level was at 1/4 of W from bottom, the (l) one 3/4 of W from bottom.

A modification of the effective crack model by Nallathambi and Karihaloo [4] was adopted in order to determine the equivalent elastic crack length at the stages of the unloading–reloading cycles. The crack length was calculated by iteration process using the formula for compliance of the three-point bend beam with a central crack. In this formula the crack length is presented as the upper limit of integral of a certain multiplication of (usually polynomial) function of geometry. The procedure was implemented in MathCAD mathematical package.

Several compliance values were taken from the unloading–reloading branches of the recorded P–d diagrams, namely the secant, unloading, reloading, and some kind of "mean" value of the latter two ones. The mean compliance was obtained as a line going through the intersections of the unloading and reloading branches of the P–d curve. Interpretation of the secant, unloading and reloading compliance and construction of the mean compliance is illustrated in Fig 4.

Values of the effective crack length presented further in this paper were computed based on the mean compliance. This approach is closest to the variant according to Jenq-Shah [5]. If the pure Nalathambi-Karihaloo model [4] based on the secant compliance was used, the effective crack lengths would be much larger than those determined from the mean compliance (and the reloading and unloading ones too).

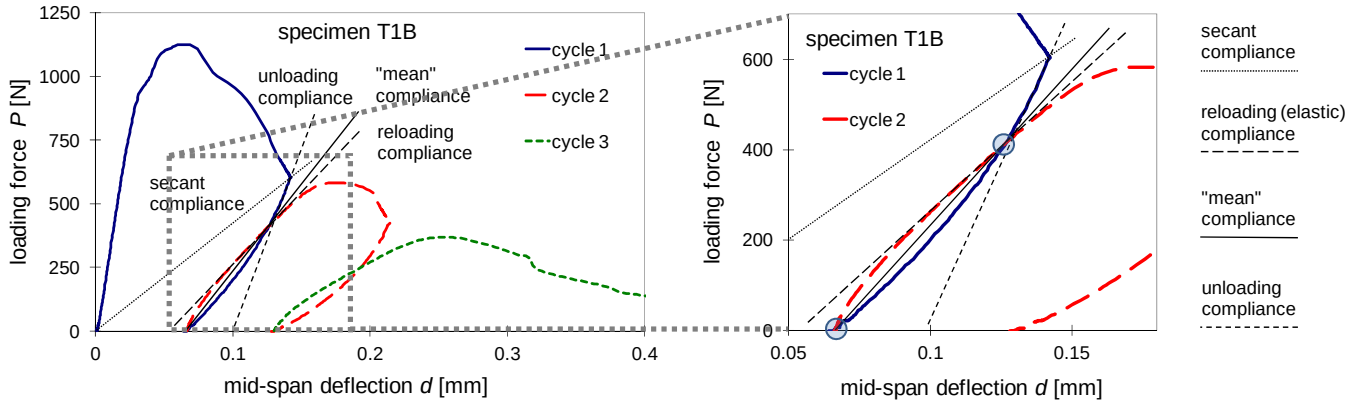

Figure 4: Variants of estimation of the specimen compliances considered for the determination of the effective crack length.

Investigation of changes in electrical resistivity during fracture process

Selected results from the evaluated concrete electrical resistivity measurements are presented herein. The measurements of resistivity were conducted before loading and after each unloading cycle until the sample broke. There was observed a gradual reduction of concrete resistivity as the loading–unloading cycles went by in the case of the specimens set with pre-dried surface (which was conducted first). Even the resistivity in the same measuring locations of the sample's intact parts was generally decreasing from cycle to cycle. Moreover, an effect of increasing wetting of the concrete surface around the Wenner probe contacts areas was observed. It is believed that the reduction of resistivity was caused by the measuring instrument repetitive wet sponge-maintained contacts with the pre-dried concrete. Therefore, the resistivity difference, $\Delta\rho$, between the crack affected and unaffected areas (and not the absolute resistivity values, ρ) was selected in order to overcome the influence of gradual probe contact areas wetting. In the second testing set, the samples were kept in bath until the test started in order to mitigate the effect of the gradual surface wetting.

The notched (n) area in the middle (M) of the sample (marking is indicated in Fig. 3a), was selected in order to study effect of the fracture propagation on the changes of electrical resistivity of the material. The average value from the left (L-n) and right (R-n) measurements in the notched area were used as a reference. Resulting parameter $\Delta\rho$ represents the resistivity reading in the middle notched area (M-n) minus the average of the intact reference areas (mean value of (L-n) and (R-n)). The relationship between the $\Delta\rho$ value and the computed effective crack length, a_{eff}, is given in Figs. 5a) and 5b) for the pre-dried and wet surface specimen sets, respectively.

Investigation of changes in ultrasound pulse passing time during fracture process

The measurements of ultrasound pulse passing time, t, were conducted before the loading begins and after each of unloading cycles similarly to the resistivity readings. The notch area (n) was of the interest herein as well. Thus, readings from the same vertical location of the specimen from its both sides were averaged (location 1 with location 3, see Fig. 3b). The time for the ultrasound wave to pass the zone affected by cracking had increasing tendency as the fracture propagated, see Figs. 6a) and 6b).

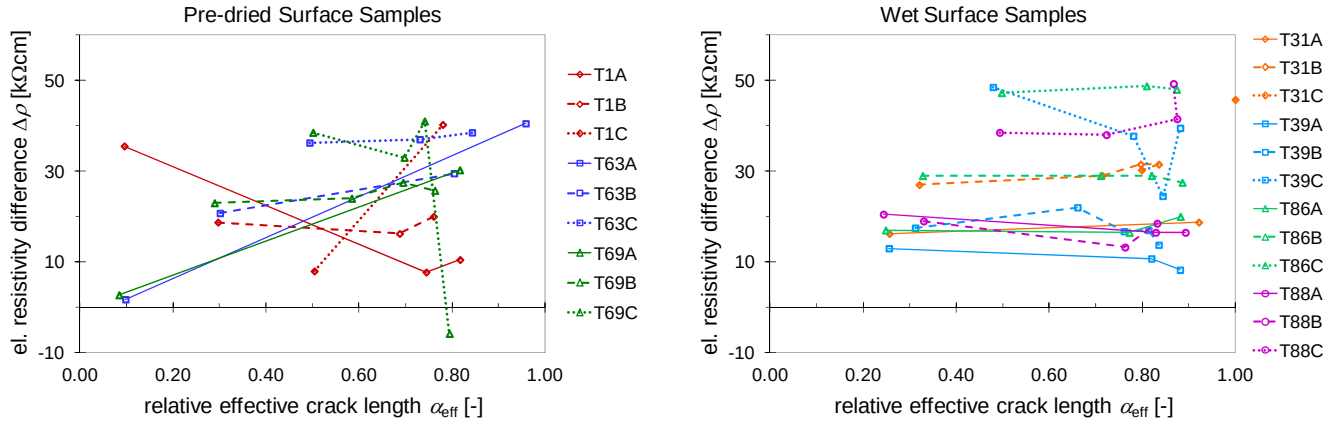

Figure 5: Relationship between the concrete electrical resistivity difference, $\Delta\rho$, and the relative effective crack length, α_{eff}, for the pre-dried (a) and the wet surface (b) samples evaluated at the notch (n) level.

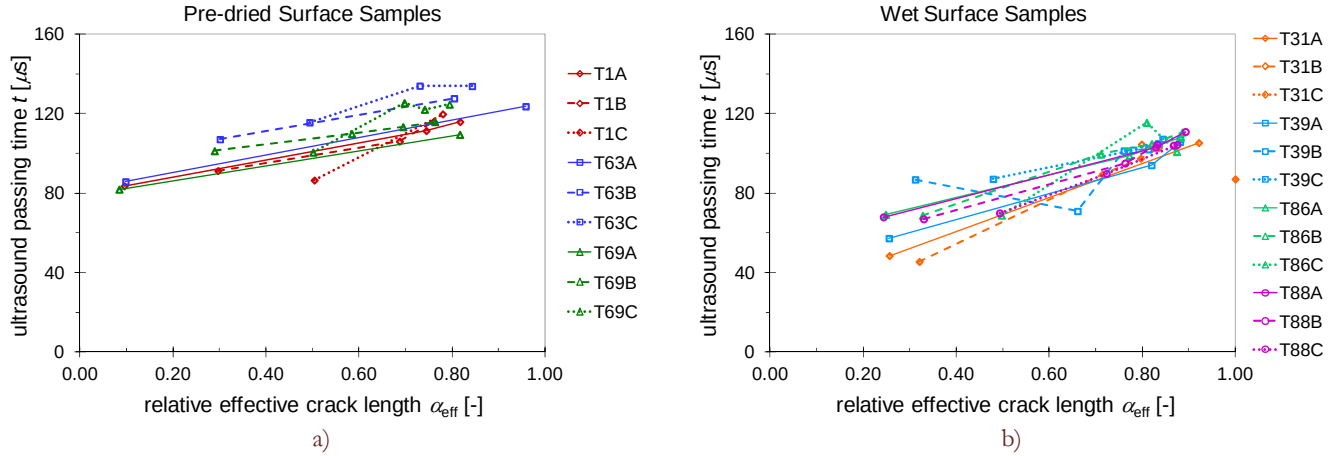

Figure 6: Relationship between the ultrasound pulse passing time, t, and the relative effective crack length, α_{eff}, for the pre-dried (a) and the wet surface (b) samples evaluated at the notch (n) level.

DISCUSSION OF RESULTS

There were two sets of samples subjected to testing in order to indicate the difference between the dried and wet surface on the results of concrete electrical resistivity as well as ultrasound pulse passing time. As was mentioned above, the samples have been cured by saturation in lime water. The pre-dried samples have been removed from the curing tank one day before testing in order to let the surface dry out. Wet samples were stored in lime-water tank until the experiment took place. These samples have been kept wet between the subsequent testing cycles by treating the surfaces with wet sponge. Both test series were conducted at different ages of the concrete specimens.
Thus, differences in conditions between the tests on the two specimen sets went from three sources: i) the time period between the specimen removal from the storage tank and the testing, ii) the existence of the wet sponge-based treatment of sample surfaces before the (resistivity) test, and iii) the age of concrete specimens. However, based on the nature of results of the conducted tests, it is not possible to precisely distinguish the effect of the individual source. Thus, the analysis is limited to the overall difference between the two specimen sets.

Electrical resistivity measurements

Fig. 5a) illustrates the overall pre-dried samples performance in terms of the difference between the resistivity value in the central (cracked) part of the specimen and the average of its values in its side (intact) parts, $\Delta\rho$, versus the relative effective

crack length, α_{eff}. Note that results from measurements in the notch level (n) are displayed. A rather disordered relationship with a large scatter was observed; however, a general trend is visible – the longer was the notch the higher was the electrical resistivity difference at the affected area, moreover, the $\Delta\rho$ value increases (in average) with increasing relative effective crack length. It is believed that the crack development created higher porosity (voids, (empty) micro-cracks) in the fracture process zone thus creating a stronger barrier for electric current to flow.
It was expected that the response of the wet specimens would be opposite to the pre-dried surface cases because micro-cracks that are created during the fracture process (expected to be filled with water) may open a path for ionic movement and thus decrease the resistivity. However, no significant relation between the resistivity difference and effective crack length was observed in the case of wet specimens; the $\Delta\rho$ values remain close to constant with the increase of the crack length. The graph is shown on the Fig. 5b). This phenomenon was observed probably due to too narrow (micro-)cracks in the fracture process zone to influence the electrical characteristics of the investigated concrete. However, the $\Delta\rho$ values of the wet surface samples were sensitive to the length of the initial notch, a_0; the resistivity difference values corresponding to different notch lengths, as well as their scatter, increased with the increase of relative notch length α_0.
In spite of the fact that the difference in electrical response between the pre-dried and the wet surface specimens was rather obvious, the values of moisture content determined after testing via standard technique (from difference of current weight and weight after drying at 110°C) were almost the same, see the last column in Tab. 1. Mean value of moisture content for the pre-dried and the wet surface samples was 6.61% and 7.74%, respectively[5]. Note that more considerable difference was expected.

Ultrasonic measurements

The ultrasound pulse passing time, t, contrary to the above-mentioned analysis on $\Delta\rho$, is showing notable correlation with the effective crack length, α_{eff}, on the pre-dried as well as the wet samples; an increasing trend is obvious, see Figs. 6a) and 6b) respectively. The distinction in t values for different notch lengths, a_0, has not been observed clearly compared to e.g. the resistivity difference of wet surface sample case (Fig. 5b)). However, again, the scatter in measured values increased with increasing notch length.

Summarizing remarks

It is worth emphasizing the following interesting findings:

- A rather significant correlation of the resistivity measurements and the effective crack length was observed only in the case of pre-dried surface specimens and not in the case of the wet surface ones.
- The relationship between the notch size and resistivity differences was observed both in the case of pre-dried as well as wet surface specimens.
- In contrast, the ultrasonic passing time has correlated significantly with crack propagation in both cases. Thus, the decrease in the velocity of waves originated by the ultrasound pulse well indicated the ongoing fracture.
- The reason for no correlation of the resistivity difference and the crack length in the case of wet surface samples may be related to too small width of the propagating crack. It is proved that only cracks wider than 30 μm allow chlorides to penetrate faster through concrete [15]. Similar phenomenon might have been present for water in voids and micro-cracks in these tests.

Alternatively to the graphs in Figs. 5 and 6, it might be convenient (e.g. in future physical analyses) to display the dependences of the measured physical properties as functions of the transverse distance between the current effective crack tip and the measuring position. This distance is marked as l_m here (see Fig. 3). Its relative value, λ_m, i.e. l_m/W, is used on horizontal axis in alternative interpretations of findings shown above. In this interpretation the dependences get opposite trends, compare Fig. 7 and Fig. 5b) or Fig. 8 and Fig. 6a).

CONCLUSIONS AND OUTLOOKS

The paper presents results of sequential fracture tests rather uniquely complemented with nondestructive measurements allowing studying the effect of crack growth on the concrete electrical resistivity and ultrasonic pulse passing time. The (changes in) resistivity values were considered as a measure for the ability of concrete to

[5] Omitting far-off measurements for specimen T86 marked with asterisk in Tab. 1.

resist penetration of aggressive species. The ultrasonic passing time values were considered as measure of damage in the area of interest.

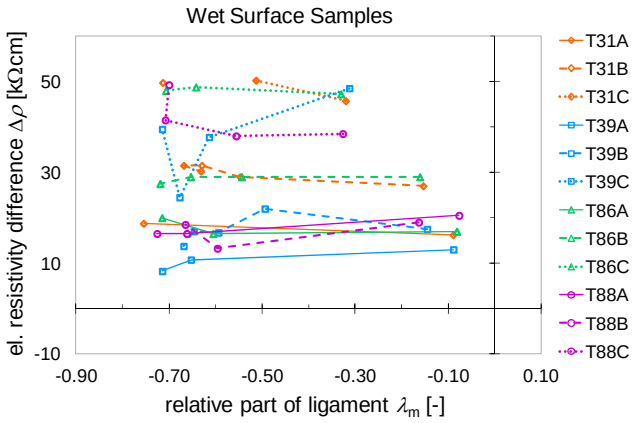

Figure 7: Relationship between the electrical resistivity difference, $\Delta\rho$, and the relative transverse distance between the effective crack tip and the measuring location, λ_m, for the wet surface samples evaluated at the notch (n) level.

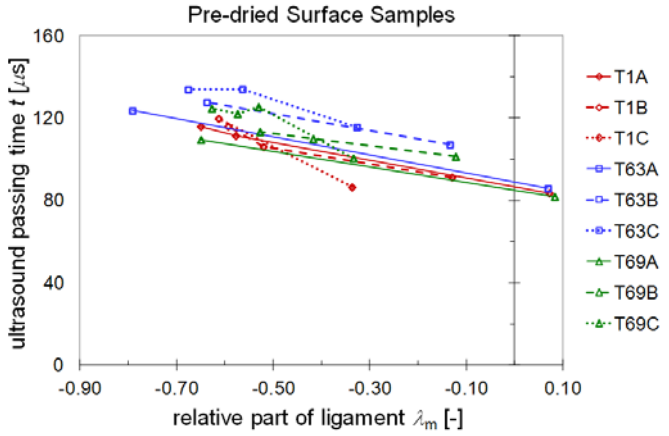

Figure 8: a) Relationship between the ultrasound pulse passing time, t, and the relative transverse distance between the effective crack tip and the measuring location, λ_m, for the pre-dried surface samples evaluated at the notch (n) level.

The study showed that the ultrasound passing time increased with the crack growth, which indicated the escalation of damage in the fracture process zone. The results of ultrasonic measurements were consistent regardless to moisture treatment of the specimen surfaces (wet or pre-dried). The studied effect of the notch length was not captured in this measurement too.

On the other hand, the results of concrete resistivity depended on the moisture treatment of the specimen surface, at least partially. The length of the effective crack seems to affect resistivity only in the case of the pre-dried surface specimens. The longer was the crack the larger was the difference between resistances in the cracked and uncracked areas. The crack length had no influence on the change of the concrete resistivity when the wet surface specimens were tested.

A hypothesis is made that the concrete resistivity of wet surface samples can be influenced only with cracks of some minimal width, in the similar manner as diffusion of chlorides through crack is influenced by its opening.

The next part of the ongoing experimental campaign shall consider both cases of the surface treatment (pre-dried as well as wet surface) to validate the presented results and the suggested hypothesis. Thus, the crack width shall be more precisely investigated during the subsequent loading–unloading cycles of the fracture test. Since the crack width is the crucial parameter for validating the hypothesis, it will be useful to have its numerical estimation as well. Linear elastic fracture mechanics will be employed for estimation of the effective crack width in the first step, then possibly some nonlinear approaches might be used.

Deeper analysis taking into account also the other considered representations of the crack length (calculated from the unloading, reloading and secant compliance) as well as the measured data from the other than only the notch (n) level of the specimens is planned.

ACKNOWLEDGEMENTS

Financial support from VŠB-Technical University of Ostrava by means of the Czech Ministry of Education, Youth and Sports through the Institutional support for conceptual development of science, research and innovations for the year 2014 is gratefully acknowledged.

REFERENCES

[1] Lindquist, W.D., Darwin, D., Browning J, Miller, G.G., Effect of cracking on chloride content in concrete bridge decks, ACI Mater J, 103(6) (2006) 467–473.

[2] Fanous, F., Wu, H., Performance of coated reinforcing bars in cracked bridge decks, J Bridge Eng, 10(3) (2005) 255–261, doi: 10.1061/(ASCE)1084-0702(2005)10:3(255).
[3] Seitl, S., Knésl, Z, Šimonová, H., Keršner, Z., Fatigue crack growth in cement based composites: Experimental aspects, In: Proceedings of the 3rd International Symposium on Life-Cycle Civil Engineering – Life-Cycle and Sustainability of Civil Infrastructure Systems, IALCCE (2012) 1314–1317.
[4] Karihaloo, B.L., Fracture mechanics and structural concrete, Longman, New York, (1995).
[5] Shah, S.P., Swartz, S.E., Ouyang, C., Fracture mechanics of structural concrete: applications of fracture mechanics to concrete, rock, and other quasi-brittle materials, Wiley, New York (1995).
[6] Bažant, Z.P., Planas, J., Fracture and size effect in concrete and other quasibrittle materials, CRC Press, Boca Raton (1998).
[7] Konečný, P., Tikalsky, P.J., Tepke, D.G., Performance evaluation of concrete bridge deck affected by chloride ingress, Transportation Research Record, 2028 (2007) 3–8, doi: 10.3141/2028-01.
[8] Bentz, D.P.,Garboczi, E.J., Lu, Y., Martys, N., Sakulich, A.R., Weiss, W.J., Modeling of the influence of transverse cracking on chloride penetration into concrete, Cement & Concrete Composites, 38 (2013) 65–74.
[9] Bentz, D.P., Clifton, J.R., Snyder, K.A., Predicting service life of chloride-exposed steel-reinforced concrete, Concr Int, 18(12) (1996) 41–47.
[10] Vořechovská, D., Teplý, B., Chromá, M., Probabilistic assessment of concrete structure durability under reinforcement corrosion attack, J Perform Constr Facil, 24(6) (2010) 571–579.
[11] Morris, W., Moreno, E.I. Sagues, A.A., Practical evaluation of resistivity of concrete in test cylinders using a Wenner array probe, Cement and Concrete Research, 26(12) (1996) 1779–1787.
[12] Ghosh, P., Hammond, A., Tikalsky, P.J., Prediction of equivalent steady state chloride diffusion coefficients, ACI Mater J, 108(1) (2011) 88–94.
[13] Veselý, V., Konečný, P., Lehner, P., Pařenica, P., Hurta, J., Žídek, L., Investigation of fracture and electrical resistivity parameters of cementitious composite for their utilization in deterioration models, Key Eng Mat, Vols. 577–578 (2014) 265–268, doi:10.4028/www.scientific.net/KEM.577-578.265.
[14] Konečný, P., Veselý, V., Lehner, P., Pieszka, D., Žídek, L., Investigation of selected physical parameters of cementitious composite during sequential fracture test, Advanced Materials Research, 969 (2014) 228–233, doi:10.4028/www.scientific.net/AMR.969.228.
[15] Djerbi, A., Bonnet, S., Khelidj, A., Baroghel-Bouny, V., Influence of traversing crack on chloride diffusion into concrete, Cement and Concrete Research, 38(6) (2008) 877–883.